Phenotypical, functional and transcriptomic comparison of two modified methods of hepatocyte differentiation from human induced pluripotent stem cells

RONG LI, YANG ZHAO, JEFFREY J. YOURICK, ROBERT L. SPRANDO and XIUGONG GAO

Division of Toxicology, Office of Applied Research and Safety Assessment, Center for Food Safety and Applied Nutrition,
U.S. Food and Drug Administration, Laurel, MD 20708, USA

Abstract. Directed differentiation of human induced pluripotent stem cells (iPSCs) into hepatocytes could provide an unlimited source of liver cells, and therefore holds great promise for regenerative medicine, disease modeling, drug screening and toxicology studies. Various methods have been established during the past decade to differentiate human iPSCs into hepatocyte-like cells (HLCs) using growth factors and/or small molecules. However, direct comparison of the differentiation efficiency and the quality of the final HLCs between different methods has rarely been reported. In the current study, two hepatocyte differentiation methods were devised, termed Method 1 and 2, through modifying existing well-known hepatocyte differentiation strategies, and the resultant cells were compared phenotypically and functionally at different stages of hepatocyte differentiation. Compared to Method 1, higher differentiation efficiency and reproducibility were observed in Method 2, which generated highly homogeneous functional HLCs at the end of the differentiation process. The cells exhibited morphology closely resembling primary human hepatocytes and expressed high levels of hepatic protein markers. More importantly, these HLCs demonstrated several essential characteristics of mature hepatocytes, including major serum protein (albumin, fibronectin and α-1 antitrypsin) secretion, urea release, glycogen storage and inducible cytochrome P450 activity. Further transcriptomic comparison of the HLCs derived from the two methods identified 1,481 differentially expressed genes (DEGs); 290 Gene Ontology terms in the biological process category were enriched by these genes, which were further categorized into 34 functional classes. Pathway analysis of the DEGs identified several signaling pathways closely involved in hepatocyte differentiation of pluripotent stem cells, including 'signaling pathways regulating pluripotency of stem cells', 'Wnt signaling pathway', 'TGF-beta signaling pathway' and 'PI3K-Akt signaling pathway'. These results may provide a molecular basis for the differences observed between the two differentiation methods and suggest ways to further improve hepatocyte differentiation in order to obtain more mature HLCs for biomedical applications.

Correspondence to: Dr Xiugong Gao, Division of Toxicology, Office of Applied Research and Safety Assessment, Center for Food Safety and Applied Nutrition, U.S. Food and Drug Administration, 8301 Muirkirk Road, Laurel, MD 20708, USA
E-mail: xiugong.gao@fda.hhs.gov

Abbreviations: A1AT, α-1-antitrypsin; AFP, α-fetoprotein; ALB, albumin; BMP4, bone morphogenetic protein 4; BP, biological process; CK18, cytokeratin 18; cRNA, complementary RNA; CYP, cytochrome P450; DAVID, Database for Annotation, Visualization, and Integrated Discovery; DE, definitive endoderm; DEG, differentially expressed gene; DEX, dexamethasone; dihexa, N-hexanoic-Try-Ile-(6)-amino hexanoic amide; FGF2, fibroblast growth factor 2; FOXA2, forkhead box protein A2; GO, gene ontology; HCA, hierarchical clustering analysis; HCM, Hepatocyte Culture Medium; HEGF, human epidermal growth factor; HGF, hepatocyte growth factor; HLC, hepatocyte-like cell; HNF4A, hepatocyte nuclear factor 4 α; iPSC, induced pluripotent stem cell; KEGG, Kyoto Encyclopedia of Genes and Genomes; LC/MS, liquid chromatography-mass spectrometry; NEAA, non-essential amino acids solution; OCT4, octamer-binding transcription factor 4; OME, omeprazole; OSM, oncostatin M; PAS, periodic acid-Schiff; PB, phenobarbital; PCA, principal component analysis; PEST, penicillin/streptomycin; PFA, paraformaldehyde; PHH, primary human hepatocyte; ROCK, Rho kinase; SOX, SRY (sex determining region Y)-box; SSEA4, stage-specific embryonic antigen-4; TRA-1-60, T cell receptor α locus; UHPLC-ESI-MS/MS, ultrahigh performance liquid chromatography-electrospray ionization tandem mass spectrometry; WME, Williams' Medium E

Introduction

The advent of induced pluripotent stem cell (iPSC) technology provides a potentially limitless source of cells for biomedical research and industrial and clinical use (1). Hepatocyte-like cells (HLCs) directly differentiated from human iPSCs facilitate the generation of genetically defined and renewable human hepatocytes (2), and therefore represent a promising alternative to primary human hepatocytes (PHHs) and hepatic cell lines.

Over the past decade, a variety of protocols have been established for the differentiation of human iPSCs into hepatocytes *in vitro*, either through viral-based expression of major hepatic transcription factors (3,4), using growth factors (5-7), small molecules (8,9), or different combinations of growth factors and small molecules (10,11) to recapitulate major signaling pathways involved in the different stages of embryonic hepatogenesis. However, directed differentiation of hepatocytes remains challenging. Although successful derivation of HLCs has been achieved through these protocols, the differentiation efficiency and reproducibility are not ideal. Often, the differentiation process needs to be optimized for different iPSC lines by fine-tuning the concentration of various growth factors or small molecules and adjusting the treatment timeline (12). More importantly, the final differentiated cells have been revealed to consist of a heterogeneous population with cells exhibiting different levels of maturity and sometimes nonspecific cells; this has led to significant uncertainty in their potential value in downstream applications (13,14). To improve the reliability of this technology, it is essential to develop a robust hepatocyte differentiation system that is highly efficient, homogeneous and reproducible.

In this study, two modified methods of hepatocyte differentiation based on existing well-known strategies were designed, and the resultant HLCs were compared phenotypically and functionally at different stages of the differentiation process. Furthermore, transcriptomic analysis was performed on the final HLCs to explore the molecular basis underlying the differences observed between the two differentiation methods.

Materials and methods

Human iPSC line and single-cell culture of iPSCs. Human iPSC cell OARSAi002-A was previously generated in our laboratory from the cord blood of a healthy non-Hispanic white male using self-replicative RNA reprogramming technology (15). Cells were maintained as a single-cell culture (no colony formation) on COAT-1 pre-coated 6-well tissue culture plates in the Cellartis DEF-CS Culture System (Takara Bio, Inc.) at 37°C in a humidified incubator supplied with 5% CO_2. For passaging, cells were dissociated into single cells with TrypLE Select Enzyme (1X) (Thermo Fisher Scientific, Inc.) and seeded at a density of $4-5 \times 10^4$ cells/cm². The cell culture medium was changed daily until the cells reached a confluence of $\sim 1.5-3.0 \times 10^5$ cells/cm², which generally occurred 3-4 days post passage. The pluripotency of the iPSCs was routinely assessed using immunocytochemistry staining of major pluripotency protein markers, including octamer-binding transcription factor 4 (OCT4), SRY (sex determining region Y)-box (SOX)2, stage-specific embryonic antigen-4 (SSEA4) and T cell receptor α locus (TRA-1-60) using a Pluripotent Stem Cell 4-Marker Immunocytochemistry Kit (cat. no. A24881) according to the manufacturer's protocol (Thermo Fisher Scientific, Inc.).

Definitive endoderm (DE) induction. DE induction was performed using the STEMdiff Definitive Endoderm Kit from STEMCELL Technologies according to the manufacturer's protocol with small modifications. On the day before DE induction (day-1), culture of the OARSAi002-A iPSC line was dissociated into single cells using TrypLE Select Enzyme (1X). Collected cells were resuspended into Cellartis DEF-CS medium supplemented with GF-1, GF-2, and GF-3 and seeded onto a 6-well tissue culture plate pre-coated with LDEV-free, hESC-qualified Matrigel (Corning Inc.) at a cell density of 2.1×10^5 cells/cm². The plate was incubated at 37°C and supplied with 5% CO_2, and the cells reached $\sim 90-100\%$ confluence by the following day. On day 0, cells were washed once with DMEM/F12 (Thermo Fisher Scientific, Inc.) and replaced with STEMdiff Endoderm basal medium with 1X supplement MR and 1X supplement CJ. Cells were then incubated with STEMdiff Endoderm basal medium with 1X supplement CJ on days 1-3, with medium replenished daily. On day 4, the protein expression of key DE markers, SOX17 and forkhead box protein A2 (FOXA2), were evaluated by immunocytochemistry staining on 4% paraformaldehyde (PFA)-fixed cells using SOX17 mouse anti-human monoclonal antibody (Abcam) and FOXA2 rabbit anti-human monoclonal antibody (Abcam), as described below.

Hepatic specification and maturation. Two approaches were employed for the hepatic specification and maturation using a combination of growth factors, cytokines and small molecules. To better compare the differentiation efficiency of the two approaches, the hepatic specification was initiated using the same source of DE cells derived above. On day 4 of DE differentiation, cells were washed with DPBS without Ca^{2+} and Mg^{2+} (Thermo Fisher Scientific, Inc.) and dissociated into single cells using StemPro Accutase Cell Dissociation Reagent (Thermo Fisher Scientific, Inc.). Cells were split into two 50-ml conical tubes before centrifugation at room temperature and 200 x g for 5 min. Collected cells were then resuspended into two different media for hepatic specification following Methods 1 and 2 (Fig. 1), as described below.

Method 1. The first differentiation method was modified based on the work by Jung *et al* (16) and Mallanna and Duncan (5). Activin A, bone morphogenetic protein 4 (BMP4) and fibroblast growth factor 2 (FGF2) were applied to guide hepatic specification of DE; hepatocyte growth factor (HGF) and oncostatin M (OSM) were further utilized to promote cell maturation into HLCs.

Briefly, DE cells in one of the 50-ml conical tubes were resuspended in RPMI Cell Differentiation Medium [including RPMI Basal Medium, 20 ng/ml BMP4 (R&D Systems) and 10 ng/ml FGF2 (Thermo Fisher Scientific, Inc.)] supplemented with 10 μM Y-27632 Rho kinase (ROCK) inhibitor (Tocris Bioscience) on day 4 and seeded onto Matrigel (Corning Inc.) pre-coated 12-well or 24-well plates (Thermo Fisher Scientific, Inc.), at a seeding density of 8×10^4 cells/cm². The RPMI Basal Medium was composed of RPMI-1640 HEPES medium, 1X B-27 Supplement with insulin, 1X Minimum Essential Medium non-essential amino acids solution (NEAA) and 1X penicillin/streptomycin (PEST) (all from Thermo Fisher Scientific, Inc.). The plate was shaken gently back and forth, then left and right to ensure even distribution of cells over the surface before being placed in the incubator overnight. The cells were replenished with RPMI Cell Differentiation Medium without ROCK inhibitor the next day and cultured for 5 days with daily medium changes. On days 9-14, the hepatic
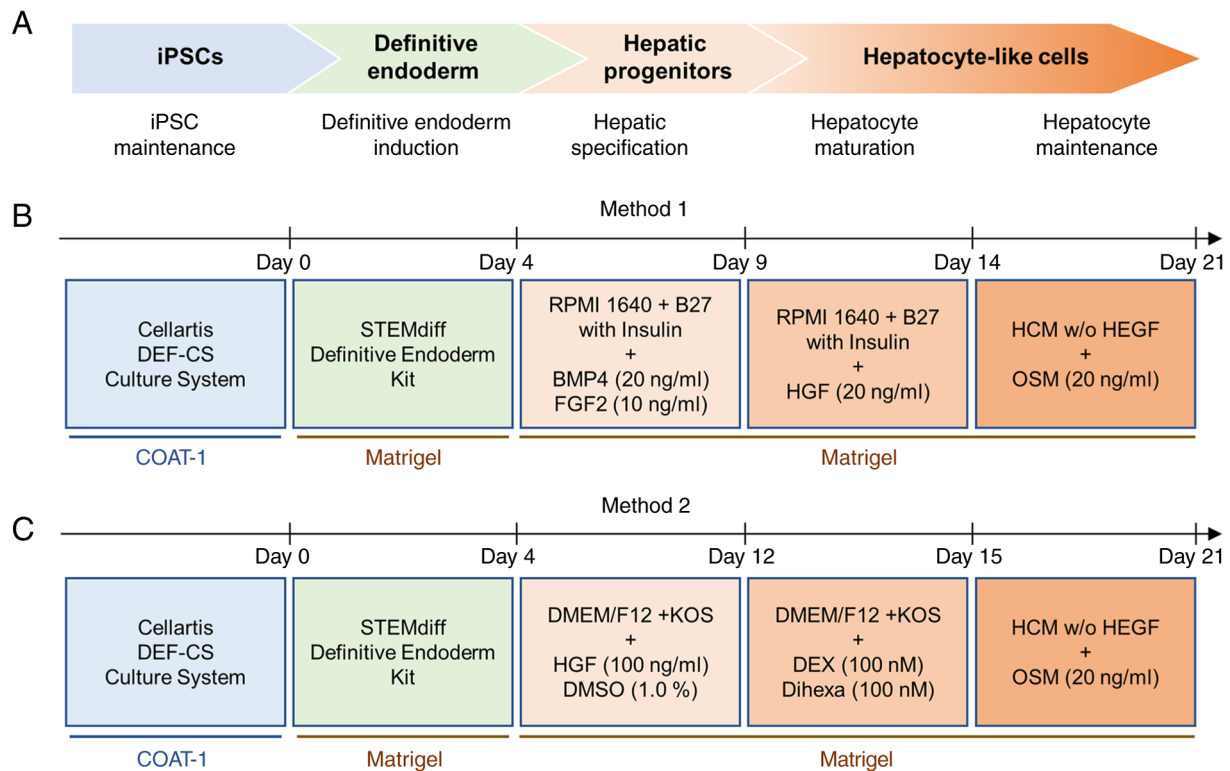
Figure 1. Schematic illustration of HLC differentiation from human iPSCs. (A) Cell states and sequential steps of the differentiation process. Differentiation timeline, media and growth factors used at each stage of (B) Differentiation Method 1 and (C) Differentiation Method 2. HCM, hepatocyte culture medium; iPSC, induced pluripotent stem cell; BMP4, bone morphogenetic protein 4; FGF2, fibroblast growth factor 2; HGF, hepatocyte growth factor; HEGF, human epidermal growth factor; OSM, oncostatin M; KOS, knockout serum replacement; DEX, dexamethasone.

progenitor cells were further cultured in RPMI Basal medium supplemented with 20 ng/ml HGF with daily medium changes. Starting from day 14, the culture medium was replaced with Hepatocyte Maintenance Medium [Lonza Hepatocyte Culture Medium (HCM) composed of 500 ml 1X HBM Basal Medium and 1X HCM SingleQuots Supplement Pack (both from Lonza Group, Ltd.), supplemented with 20 ng/ml OSM (R&D Systems)]. The SingleQuots Supplement Pack contained 0.5 ml transferrin, 0.5 ml ascorbic acid, 0.5 ml human epidermal growth factor (HEGF), 0.5 ml insulin, 0.5 ml hydrocortisone, 10.5 ml BSA (fatty acid-free) and 0.5 ml genta-micin-amphotericin-1000. All components in the SingleQuots Supplement Pack were added to the medium except for HEGF. The cells were further cultured for 7 days with daily medium changes. After day 21, Hepatocyte Maintenance Medium was replenished every 2-3 days for further maintenance of the differentiated HLCs.

Method 2. The second differentiation method was modified based on the work by Basma *et al* (17), Carpentier *et al* (10), and Siller *et al* (8). DMSO and HGF were employed to guide the hepatic specification, followed by hepatic maturation promoted by dexamethasone (DEX), N-hexanoic-Try-Ile-(6)-amino hexanoic amide (dihexa) and OSM.

Briefly, DE cells in the second 50-ml conical tube were resuspended in Hepatic Specification Medium, composed of Hepatocyte Differentiation Basal Medium supplemented with 100 ng/ml HGF, 1% DMSO as well as 10 μM Y-27632 and seeded onto Matrigel pre-coated 12-well or 24-well plates,

at a seeding density of 8×10^4 cells/cm^2. The Hepatocyte Differentiation Basal Medium was composed of DMEM/F12, 10% KnockOut Serum Replacement (Thermo Fisher Scientific, Inc.), 1X NEAA, 1X PEST and 1X GlutaMAX Supplement (Thermo Fisher Scientific, Inc.). The plate was gently shaken as above to ensure even distribution of cells over the entire surface and then incubated overnight. The following day, the medium was replaced with fresh Hepatic Specification Medium without ROCK inhibitor, and the cells were cultured for a further 7 days with daily medium changes. On days 12-14, the resultant hepatic progenitors were further cultured in Hepatic Maturation Medium (Hepatocyte Differentiation Basal Medium supplemented with 100 nM DEX and 100 nM dihexa) for 3 days with a daily medium change. Starting from day 15, the cell culture medium was changed to Hepatocyte Maintenance Medium, as described in Method 1. The cells were continually cultured for 6 days with daily medium changes. After day 21, Hepatocyte Maintenance Medium was replaced every 2-3 days for further maintenance of the differ-entiated HLCs.

Immunocytochemistry staining. Cells generated at different stages of the differentiation process, such as DE cells and HLCs, were fixed with 4% PFA for 20 min at room temperature, rinsed with DPBS with Ca^{2+} and Mg^{2+}, and permeabilized with 0.3% Triton X-100 in DPBS for 15 min. Cells were then incubated with Image-iT FX signal enhancer (Thermo Fisher Scientific, Inc.) for 40 min at room temperature, followed by incubation with primary antibodies, including FOXA2

rabbit anti-human monoclonal antibody (cat. no. ab108422; Abcam; 1:50), SOX17 mouse anti-human monoclonal antibody (cat. no. ab84990; Abcam; 1:50), hepatocyte nuclear factor 4 α (HNF4A) rabbit anti-human polyclonal antibody (cat. no. HPA004712; Sigma-Aldrich; Merck KGaA; 1:50), cytochrome P450 (CYP)3A4 mouse anti-human monoclonal antibody (cat. no. 67110; ProteinTech Group, Inc.; 1:50), α-fetoprotein (AFP) mouse anti-human monoclonal antibody (cat. no. MAB1368; R&D Systems; 1:20), albumin (ALB) mouse anti-human monoclonal antibody (cat. no. MAB1455; R&D Systems; 1:20), cytokeratin 18 (CK18) mouse anti-human monoclonal antibody (cat. no. MAB7619; R&D Systems; 1:20), and α-1-antitrypsin (A1AT) mouse anti-human monoclonal antibody (cat. no. MAB1268; R&D Systems; 1:20). Cells were incubated with primary antibodies overnight at 4°C in a humidified environment. The following day, cells were washed three times with DPBS and incubated with the corresponding secondary antibodies conjugated to Alexa Fluor 488 or Alexa Fluor 555 fluorophores (Thermo Fisher Scientific, Inc.) for 2 h at room temperature. The cell nuclei were counterstained with Hoechst 33342 at room temperature for 15 min, and the cell images were captured using the EVOS FL imaging system (Thermo Fisher Scientific, Inc.) with a 20X objective lens and RFP, GFP and DAPI filters. The expression rates of marker proteins and the mean fluorescence intensities of marker protein expression in the cells were quantified using ImageJ version 1.41 (National Institutes of Health) (18). To calculate the expression rates of SOX17 and HNF4A, four fields were randomly chosen for cell counting, and a total of ~3,600 nuclei were counted for SOX17 and ~1,200 for HNF4A. For marker protein expression of HLCs, average fluorescence intensity from four randomly chosen areas was calculated.

Serum protein secretion. HLCs cultured in 12-well plates were incubated in 1 ml/well of Hepatocyte Maintenance Medium for 24 h; the cell culture supernatant was collected and stored at -80°C until required. Wells without cells were included as blank controls. ELISA kits (all from Abcam) were used to determine the concentrations of ALB (cat. no. ab108788), fibronectin (cat. no. ab229398), and A1AT (cat. no. ab229417) in the cell culture supernatant following the manufacturer's instructions. Results were normalized to protein quantity in each well and presented as the mean ± standard deviation of four independent experiments.

Protein extraction and quantification. Cells were lysed in cold Pierce RIPA lysis buffer (Thermo Fisher Scientific, Inc.) supplemented with 1X Halt Protease Inhibitor Cocktail (Thermo Fisher Scientific, Inc.) for 5 min. The supernatant was collected after centrifugation at room temperature and 1,600 x g for 10 min. Total protein was quantified using a Pierce BCA Protein Assay kit (Thermo Fisher Scientific, Inc.) according to the manufacturer's protocol.

Urea synthesis and release. HLCs cultured in 24-well plates were treated with different concentrations of NH_4Cl (0, 2 or 5 mM) in 1 ml Hepatocyte Maintenance Medium for 24 h. The cell culture supernatant was collected and analyzed for urea levels using a Urea Assay kit (cat. no. 83362; Abcam) according to the manufacturer's protocol. Wells without cells

were included as blank controls. Results were normalized to protein quantities and presented as the mean ± standard deviation of three independent experiments.

Periodic acid-Schiff (PAS) staining. Differentiated HLCs were fixed with 4% PFA as above and stained with a PAS staining kit (Sigma-Aldrich; Merck KGaA) to visualize glycogen storage following the manufacturer's instructions. Phase-contrast images were taken using a BZ-X810 microscope from Keyence Corporation with a 20X objective lens.

Cytochrome P450 activity assay. CYP metabolic activity of HLCs was analyzed following an adapted version of a previously described protocol (19). Briefly, HLCs cultured in 12-well tissue culture plates were untreated or treated with omeprazole (OME, 100 μM) or phenobarbital (PB, 500 μM) for 72 h, with medium replenished every day. Cells were carefully washed twice with prewarmed phenol-red free Williams' Medium E (WME; Sigma-Aldrich; Merck KGaA) supplemented with 0.1% PEST. The assay was initiated by adding 500 μl warm CYP activity assay medium comprised of WME, 0.1% PEST, 25 mM HEPES, 2 mM L-Glutamine, and 1x CYP substrate cocktail prepared in the laboratory. The 1x CYP substrate cocktail contained phenacetin (10 μM), bupropion (10 μM), mephenytoin (50 μM), diclofenac (10 μM), bufuralol (10 μM) and midazolam (5 μM). After incubation at 37°C for 2 h, 100 μl of the supernatant was collected for ultrahigh performance liquid chromatography-electrospray ionization tandem mass spectrometry (UHPLC-ESI-MS/MS) analysis of the specific metabolites of the six CYP variants: acetaminophen (CYP1A), OH-bupropion (CYP2B6), 4-OH-mephenytoin (CYP2C19), 4-OH-diclofenac (CYP2C9), OH-bufuralol (CYP2D6) and 1-OH-midazolam (CYP3A). An Agilent 1290 Infinity II LC system (Agilent Technologies, Inc.) was used in the present study. Chromatographic separation was performed on an Agilent ZORBAX SB-C18 column (1.8 μm, 2.1x50 mm). Detection was performed using an Agilent 6460 Triple Quadrupole Mass Spectrometer fitted with electrospray ionization in positive ion mode (Agilent Technologies, Inc.). Agilent MassHunter Qualitative Analysis software version B.07.00 (Agilent Technologies, Inc.) was used to integrate the peak areas of the analytes of interest. A metabolite cocktail of all six metabolites at different dilutions was included in each liquid chromatography-mass spectrometry (LC/MS) run to create a standard curve to determine the metabolite level in each sample. The metabolite concentration was normalized to protein quantity in each well, and to the assay duration (2 h).

RNA extraction and quality assurance. Cells were harvested on days 17 and 21 of hepatocyte differentiation from Methods 1 and 2 and stored at -80°C before RNA extraction. Cells were lysed in RLT buffer (Qiagen GmbH) and homogenized using QIAshredder (Qiagen GmbH). Total RNA was extracted from the cell lysates using an EZ1 RNA Cell Mini Kit (Qiagen GmbH) on EZ1 Advanced XL automated RNA purification instrument (Qiagen GmbH) following the manufacturer's instruction. An on-column DNase digestion step was included to remove potential DNA contamination. The total RNA and purity (260/280 nm) were subsequently

measured using a NanoDrop 2000 UV-Vis spectrophotometer (NanoDrop Products). The integrity of RNA samples was further assessed using the Agilent 2100 Bioanalyzer with the RNA 6000 Nano Reagent Kit (Agilent Technologies) to obtain the RNA integrity number.

Transcriptomic analysis using microarrays. Global gene expression profiling of HLCs derived from differentiation Methods 1 and 2 was conducted using GeneChip PrimeView Human Gene Expression Arrays (Affymetrix; Thermo Fisher Scientific, Inc.) as described previously (20,21). Total RNA isolated from the cell samples was processed using GeneChip 3' IVT PLUS Reagent Kit (Affymetrix; Thermo Fisher Scientific, Inc.) following the manufacturer's protocol. Briefly, single-stranded cDNA was generated from 100 ng total RNA, which was then converted to double-stranded cDNA. Subsequently, the complementary RNA (cRNA) was synthesized through *in vitro* transcription with biotinylated UTP and CTP, using the second strand of the double-stranded cDNA as the template.

The biotin-labeled cRNA was then purified, fragmented and hybridized to the arrays in the GeneChip Hybridization Oven 645 (Affymetrix; Thermo Fisher Scientific, Inc.). After hybridization, the array chips were stained and washed using the GeneChip Fluidics Station 450. The chips were then scanned using GeneChip Scanner 3000 7G and the scanned image (.DAT) files were further processed using GeneChip Command Console software version 4.0 (Affymetrix; Thermo Fisher Scientific, Inc.) to produce cell intensity (.CEL) files. All arrays were assessed for data quality using Expression Console software version 1.3 (Affymetrix; Thermo Fisher Scientific, Inc.) before further data analysis. The dataset has been deposited in Gene Expression Omnibus (GEO; http://www.ncbi.nlm.nih.gov/geo/) of the National Center for Biotechnology Information with accession no. GSE187011.

Microarray data processing and analysis. The robust multi-array average algorithm (22) integrated into the Affymetrix Expression Console software version 1.3 was used to summarize values of individual probes belonging to one probe set in the CEL files. Unsupervised principal component analysis (PCA) and hierarchical clustering analysis (HCA) on normalized data from all cell samples were conducted using the ArrayTrack software system developed by the U.S. Food and Drug Administration (23) to explore similarities and differences among the samples. HCA clustering was based on Ward's minimum variance linkage algorithm.

To identify differentially expressed genes (DEGs), statistical analysis between two experimental groups was conducted using Affymetrix Transcriptome Analysis Console software 4.0, based on ebayes ANOVA. For each comparison, the fold change of every annotated gene, together with their ANOVA P-value or false discovery rate, was used to identify DEGs with cutoff values indicated in the text.

Gene ontology (GO) and pathway analysis. The online tool Database for Annotation, Visualization, and Integrated Discovery (DAVID) (https://david.ncifcrf.gov/) (24,25) was used for GO analysis of the identified DEGs to find GO terms overrepresented in the biological process (BP) category (GOTERM_BP_DIRECT) and to identify Kyoto Encyclopedia of Genes and Genomes (KEGG) pathways overrepresented by the DEGs. The whole genome of *Homo sapiens* was used as the background for analysis. Enrichment of GO terms was statistically determined using the default settings in DAVID. The enriched GO terms were then categorized into major GO classes using the online tool CateGOrizer (https://www.animalgenome.org/tools/catego/) based on the GO Slim subset (www.geneontology.org/GO.slims.shtml).

Statistical analysis. Data are presented as the mean ± standard deviation. Statistical analysis of the phenotypical and functional data was performed using GraphPad Prism version 9.2.0 (GraphPad Software Inc.). For the serum protein secretion and CYP activity data, a Student's t-test was used to analyze the statistical significance of differences between two groups. For the urea synthesis and release data, one-way ANOVA was performed followed by a Bonferroni post hoc test.

Results

Single-cell culture of human iPSCs improves cell homogeneity. To obtain a homogenous cell population of human iPSCs for HLC differentiation, the cells were cultured in the Cellartis DEF-CS Culture System. Unlike the traditional colony-forming culture system (e.g., culturing iPSCs using E8 medium or mTeSR medium on Matrigel-coated tissue culture plates) (26), the DEF-CS culture system supports single-cell growth (no colony formation) during cell culture. Additionally, instead of using EDTA to passage the cells, which results in small aggregates of cells, TrypLE Select Enzyme was used to dissociate the monolayer culture of cells into single cells for passaging. Dissociated cells were then seeded onto COAT-1 pre-coated tissue culture plates at a sub-confluency rate. The cells became denser with proliferation and evolved typical undifferentiated stem cell morphology; namely, tightly packed, round cells with large and notable nucleoli, and a high nucleus to cytoplasm ratio (Fig. 2A, day 0). Immunocytochemistry staining demonstrated that these cells expressed high levels of major pluripotency protein markers, such as OCT4, SSEA4, TRA-1-60, and SOX2 (Fig. 3A).

Homogeneous definitive endoderm induction. DE induction from iPSCs represents a crucial first step for subsequent efficient hepatic differentiation. To achieve highly efficient and consistent DE induction, DE induction was performed using the STEMdiff Definitive Endoderm Kit. After single-cell dissociation of iPSCs with TrypLE Select Enzyme, cells were plated on Matrigel-coated 6-well tissue culture plates with ROCK inhibitor. The cells formed a subconfluent monolayer the next day, thus making it possible for the growth factors to act homogeneously on the stem cell population. During the 4 days of DE induction, the cell morphology kept evolving, and a confluent monolayer of homogeneous DE cells with a spiky shape was obtained at the end of the induction without any aggregates or multicellular structures (Fig. 2A). Each well of a 6-well tissue culture plate contained ~2.5x10^6 of DE cells. Further immunocytochemistry staining demonstrated that these cells expressed high levels of DE marker proteins FOXA2 and SOX17, with an expression rate for SOX17 at 91.9±6.5% (Fig. 3B). OCT4, a pluripotency marker,
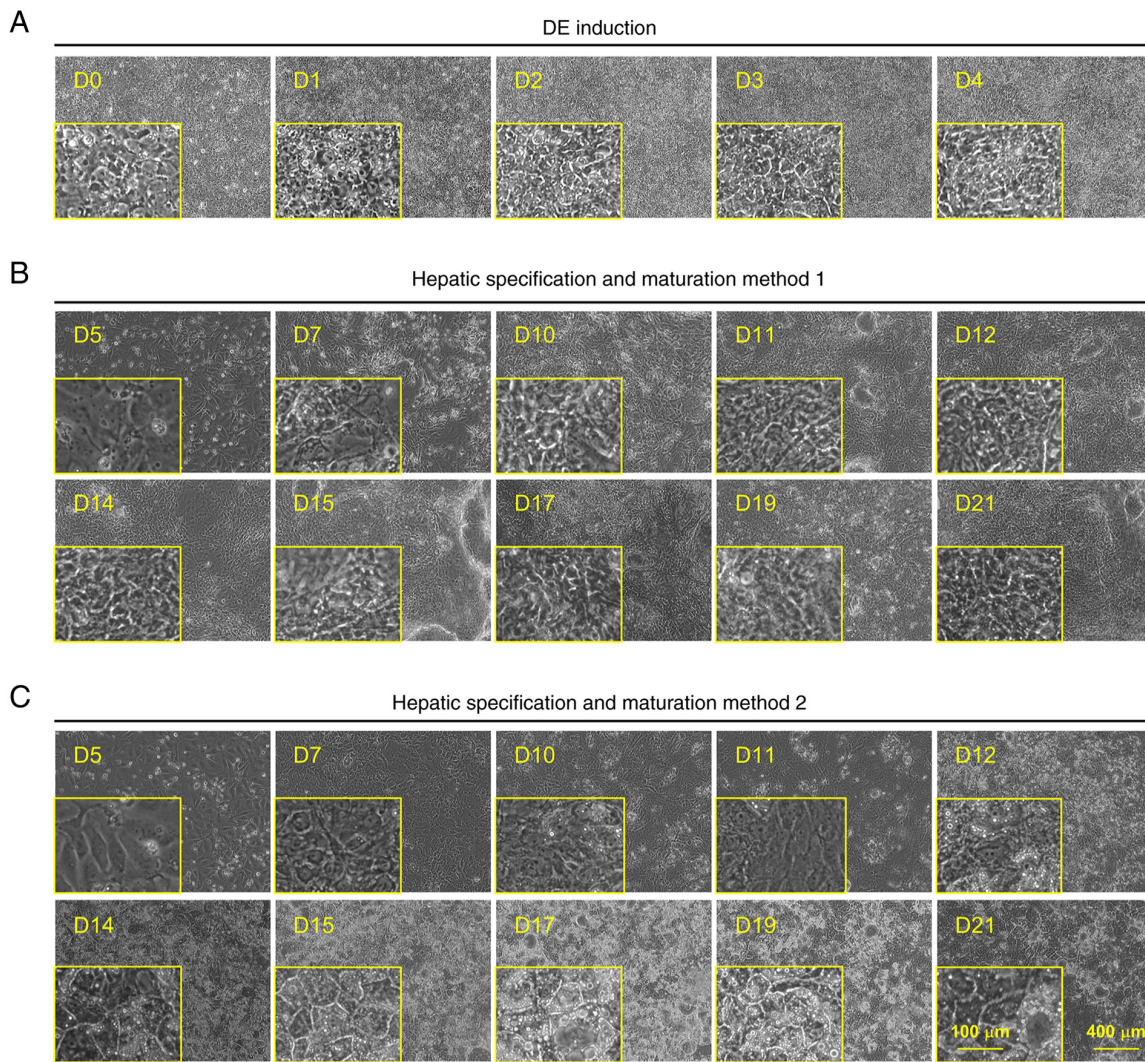
Figure 2. Representative images showing sequential morphological changes during the process of HLC differentiation. (A) DE induction. Hepatic specification and HLC maturation of (B) Method 1 and (C) Method 2. Scale bar, 400 μm; inset scale bar, 100 μm. D, day; DE, definitive endoderm.

was also stained for, but showed negative expression (data not shown), indicating a highly efficient induction of DE cells.

Hepatic specification and hepatocyte maturation. To determine a more efficient method for hepatic specification and hepatocyte maturation, and to obtain highly homogeneous functional HLCs, two modified strategies were designed and evaluated (Fig. 1). The sequential phase-contrast cell images during hepatic specification and hepatocyte maturation process of Method 1 and 2 are shown in Fig. 2B and C, respectively. In both methods, the replated DE cells attached to the Matrigel-coated tissue culture plates adequately the next day. All the cells spread out and covered 85-95% of the surface area of the wells. Rapid cell growth was observed in cells from both differentiation methods in the next several days. The cells in Method 2 reached confluence and became growth arrested at the end of hepatic specification. In contrast, cell proliferation continued into the hepatocyte maturation stage for cells in Method 1. In both methods, a gradual cell morphology change was observed. The cells transformed from the spiky shape of DE cells to a polygonal shape, typical of hepatic progenitors. Although they started from the same source of DE cells,

substantial differences were observed with regard to the changes in cell morphology. The cells from Method 1 generally demonstrated a mild and slow change in morphology. The final differentiated HLCs displayed a relatively heterogeneous and immature phenotype of a compact, small-sized polygonal shape with weak intercellular junctions and few lipid droplets in the cytoplasm. On the contrary, a dramatic cell change in morphology was observed in cells derived from Method 2 by day 12, the end of the hepatic specification. The cells exhibited an enlarged polygonal shape, apparent intercellular junctions and visible lipid droplets in the cytoplasm. During the next 9 days of hepatocyte maturation and maintenance, the cell morphology kept evolving. On day 21, the final differentiated HLCs from Method 2 displayed a highly homogeneous morphology closely resembling that of PHHs; a distinct cuboidal shape, a high nucleus-to-cytoplasm ratio, sometimes binucleated, bright intercellular junctions and the presence of prominent lipid droplets in the cytoplasm.

Immunocytochemistry staining of hepatic marker proteins was performed to assess the cell maturity of differentiated HLCs. Cells on day 21 from both differentiation methods demonstrated characteristic nuclear staining of HNF4A, and
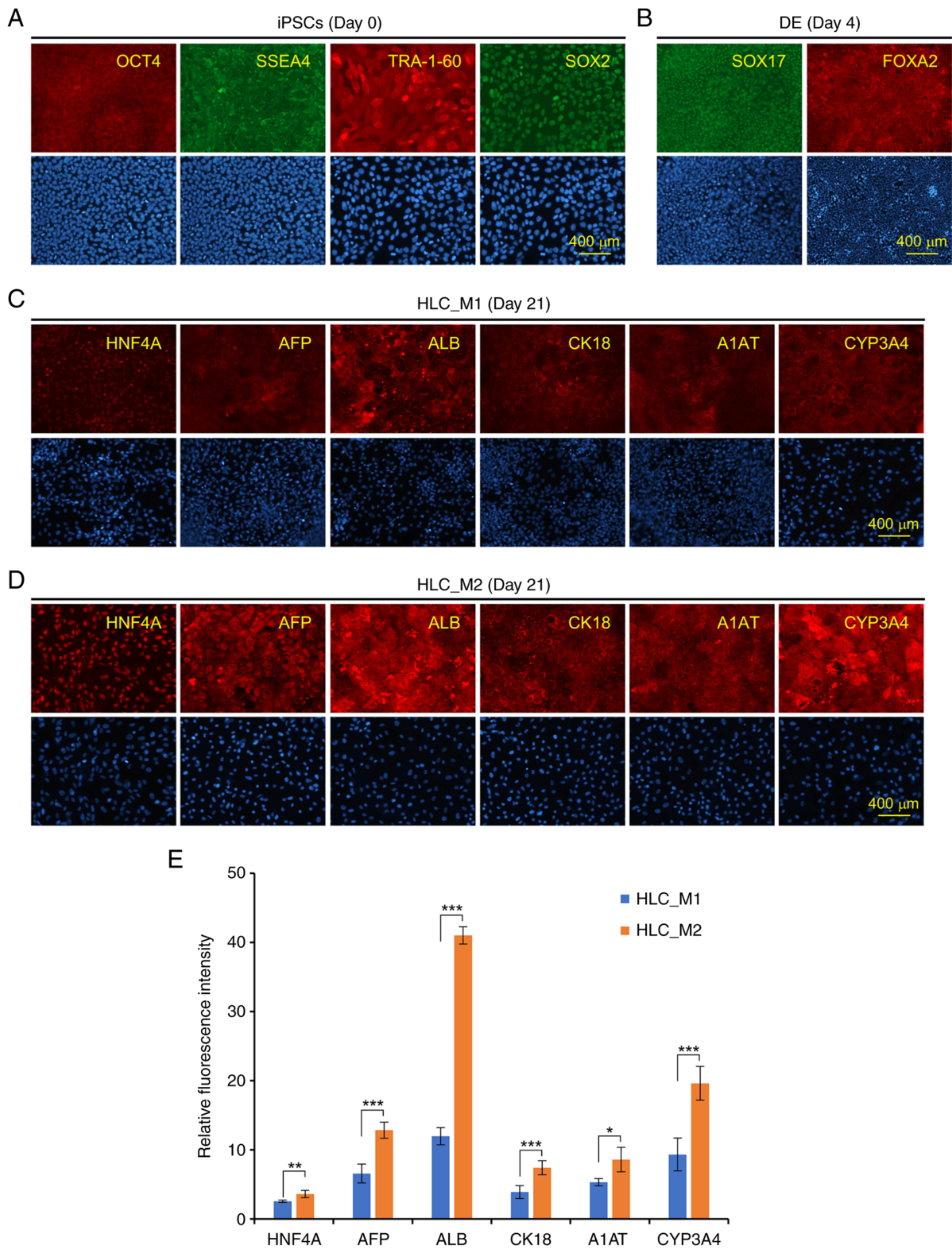
Figure 3. Immunocytochemistry staining showing the expression of characteristic stage-specific protein markers at major stages of HLC differentiation. (A) OCT4, SSEA4, TRA-1-60, and SOX2 for iPSCs. (B) SOX17 and FOXA2 for DE cells. HNF4A, AFP, ALB, CK18, A1AT, and CYP3A4 for HLCs derived from (C) Method 1 and (D) Method 2. Scale bar, 400 μm. (E) Quantification of fluorescence intensity of hepatic protein marker immunostaining. n=4, *P<0.05, **P<0.01, ***P<0.001 using a two tailed Student's t-test. HLC, hepatocyte-like cell; DE, definitive endoderm; iPSC, induced pluripotent stem cell.

cytoplasm expression of AFP, ALB, CK18, A1AT and CYP3A4 (Fig. 3C and D). Although there was no significant difference (P=0.10) in the expression rate of HNF4A in HLCs differentiated from the two methods (94.0±2.6% vs. 97.1±2.4% for cells derived from Method 1 and 2, respectively, a significant

difference in immunofluorescence intensity was detected. The mean fluorescence intensity of HNF4A in HLCs derived from Method 1 was 2.55±0.16 vs. 3.61±0.52 in HLCs obtained from Method 2 (P<0.01). Furthermore, HLCs derived from Method 2 showed significantly stronger immunofluorescence
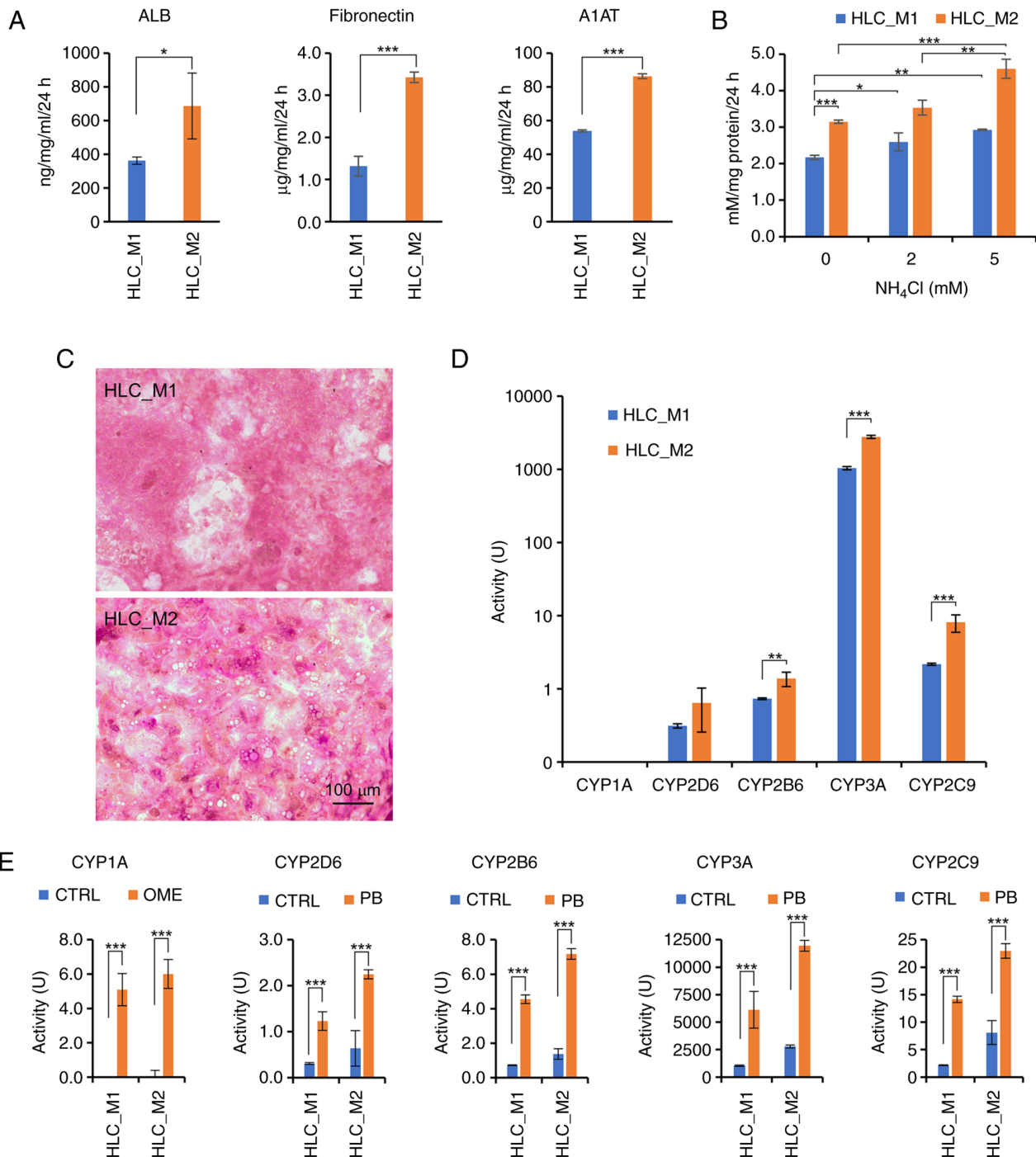
Figure 4. Functional characterization of HLCs. (A) Secretion of serum proteins ALB, fibronectin and A1AT. (B) Urea synthesis and release upon incubation with different concentrations of NH4Cl. (C) Periodic acid-Schiff staining showing glycogen storage. Scale bar, 100 μm. (D) Basal activities of CYP1A, CYP2D6, CYP2B6, CYP3A, and CYP2C9. (E) Induction of CYP1A, CYP2D6, CYP2B6, CYP3A and CYP2C9, respectively, after treatment with OME or PB. For CYP activity, 1 unit (U)=1 pmol metabolite/mg protein/h, and the metabolites are acetaminophen, 1'-hydroxy bufuralol, hydroxy bupropion, 1'-hydroxy midazolam and 4'-hydroxy diclofenac for CYP1A, CYP2D6, CYP2B6, CYP3A, and CYP2C9, respectively. All values are presented as the mean ± standard deviation. n=4 for serum protein secretion and CYP activity, and n=3 for urea synthesis. *P<0.05, **P<0.01, ***P<0.001. HLC, hepatocyte-like cell; ALB, albumin; A1AT, α-1-antitrypsin; CYP, cytochrome P450; OME, omeprazole; PB, phenobarbital; HLC_M1, HLCs derived from method 1; HLC_M2, HLCs derived from method 2.

signals for all other five hepatic markers (AFP, ALB, CK18, A1AT and CYP3A4) compared with cells from Method 1 (Fig. 3E).

Hepatic functional characterization of HLCs. Next, whether the HLCs differentiated from both Methods 1 and 2 displayed key hepatic functional characteristics was assessed. Serum protein secretion is one of the common indicators of hepatic maturation; therefore, the ability of HLCs to secrete ALB, fibronectin and A1AT was assessed by ELISA. As shown in Fig. 4A, HLCs from both methods secreted large amounts of ALB, fibronectin and A1AT into the cell culture medium, indicating hepatic maturation of the differentiated cells. In comparison, the secretion levels of ALB, fibronectin, and

A1AT from HLCs generated from Method 2 were 1.6, 1.9 and 2.6-fold higher than those of HLCs derived from Method 1.

The urea cycle is a crucial detoxification pathway that converts ammonia into urea. Since urea is almost exclusively produced by the liver, ureogenic capacity is commonly used as an indicator of a differentiated hepatic phenotype. As demonstrated in Fig. 4B, HLCs from both methods synthesized and released urea into the cell culture medium. The basal secretion of urea in differentiated HLCs derived from Method 2 was ~1.4-fold higher than that of cells derived from Method 1. Upon treatment of NH_4Cl, the urea secretion increased significantly from cells derived from both methods in a dose-dependent manner.

Another essential function of hepatocytes *in vivo* is the ability to store glycogen. After being stained with PAS and counterstaining with hematoxylin and eosin, HLCs derived from both Methods 1 and 2 showed extensive cytoplasmic staining (pink to purple), indicative of glycogen storage in the cells (Fig. 4C).

Hepatocytes are capable of clearing xenobiotics via metabolism through CYP isoenzymes (27). Therefore, CYP activity is the most critical attribute of hepatocytes for toxicological applications (28). UHPLC-ESI-MS/MS analysis was used to assess the basal level and the induction level activity of major CYP isoenzymes in HLCs derived from both differentiation methods on day 21. HLCs obtained from Method 2 demonstrated significantly higher basal activities of CYP2B6, CYP3A and CYP2C9 isoenzymes compared with the cells derived from Method 1 (Fig. 4D). The basal activities of CYP1A and CYP2C19 in cells from both methods were below the detection limit. However, activities of CYP1A, CYP2D6, CYP2B6, CYP3A and CYP2C9 were significantly increased in HLCs after treatment with OME or PB for 72 h, with a more dramatic increase in HLCs derived from Method 2 (Fig. 4E).

Transcriptomic characterization of HLCs. To obtain an unbiased assessment and comparison of the HLCs differentiated from Method 1 and 2, whole transcriptome gene expression analysis on cells at early maturation (day 17) and late maturation (day 21) stages of hepatocyte differentiation was performed and this was further compared with PHHs. All RNA samples passed the RNA quality analysis with an RNA integrity number ≥8.0. Before data analysis, all arrays in this study were assessed for data quality with all quality assessment metrics (including spike-in controls during target preparation and hybridization) within default boundaries.

PCA of the microarray data (Fig. 5A) showed that the HLCs derived from differentiation Method 1 and 2 were located close to each other along the axis of the first principal component (PC1), accounting for 80.3% of the total variance among the samples. However, they were separated from each other along the axis of the second principal component (PC2), which accounted for 9.2% of the variance among the samples. The biological replicates of HLCs at day 17 and 21 from Method 1 and 2 were clustered together. The transcriptomic datasets of PHHs reported previously (21) were also included in the graph for comparison, which were far separated from HLCs of both Method 1 and 2 along the axis of PC1. Consistent with the PCA plot (Fig. 5A), HCA clustered all the samples into respective cell groups (Fig. 5B).
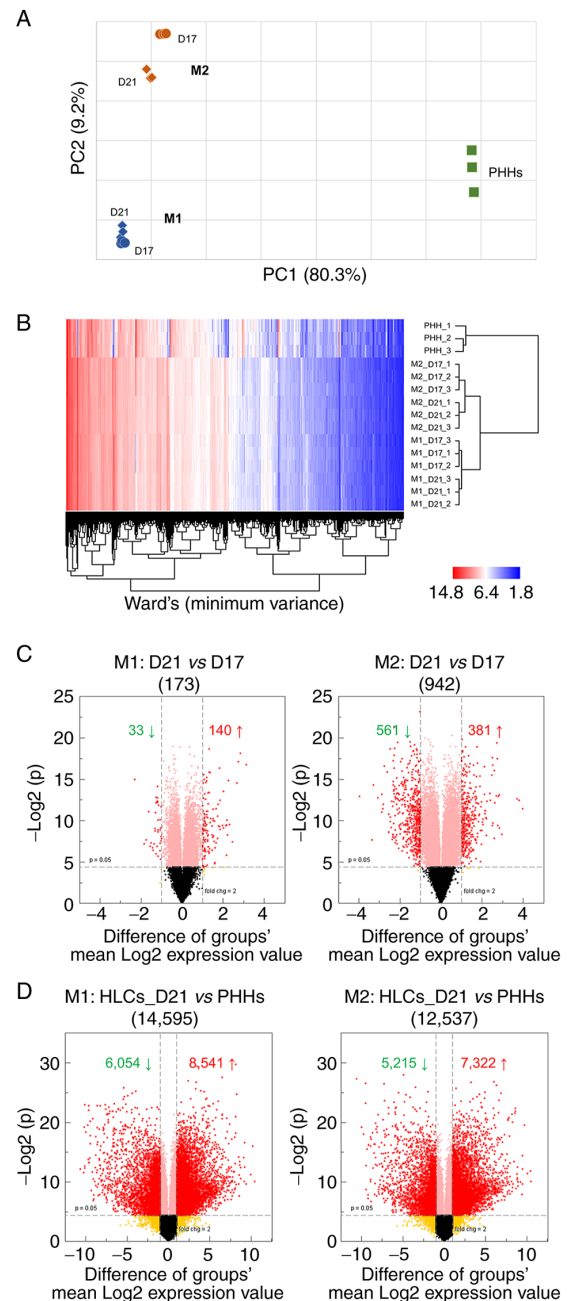
Figure 5. Global gene expression of HLCs derived from hepatocyte differentiation Method 1 (M1) and Method 2 (M2). (A) Principal component analysis using all probe sets on the array to cluster samples based on their similarities in global gene expression level. The two axes PC1 and PC2, represent the first two principal components identified by the analysis. The percentage contribution of each component to the overall source of variation is included in the parenthesis following the component name. The cell samples collected at different stages of hepatocyte differentiation from different differentiation methods are color-coded, as shown in the graph. HLCs were collected on day 17 (D17, round) and day 21 (D21, diamond) after differentiation by Method 1 (blue) and Method 2 (red). PHHs (green square) were also included for comparison. (B) Hierarchical cluster analysis based on all genes. Expression data are in log2 scale and color-coded as shown in the scheme in the bottom right corner. The dendrogram on the bottom shows clusters of genes, while the dendrogram on the right shows clusters of samples. (C) Volcano plots showing the DEGs between HLCs on D17 and 21 by differentiation Method 1 and differentiation Method 2. (D) Volcano plots showing the DEGs between PHHs and HLCs (D21) derived from differentiation Method 1 and differentiation Method 2. All DEGs are shown as red dots. Downregulated genes are on the top-left corner with numbers denoted by green arrow and upregulated genes are on the top-right corner denoted by red arrow. The total number of DEGs is included in the parenthesis under the title of the panel. HLC, hepatocyte-like cell; PC, principal component; PHHs, primary human hepatocytes; DEG, differentially expressed gene.
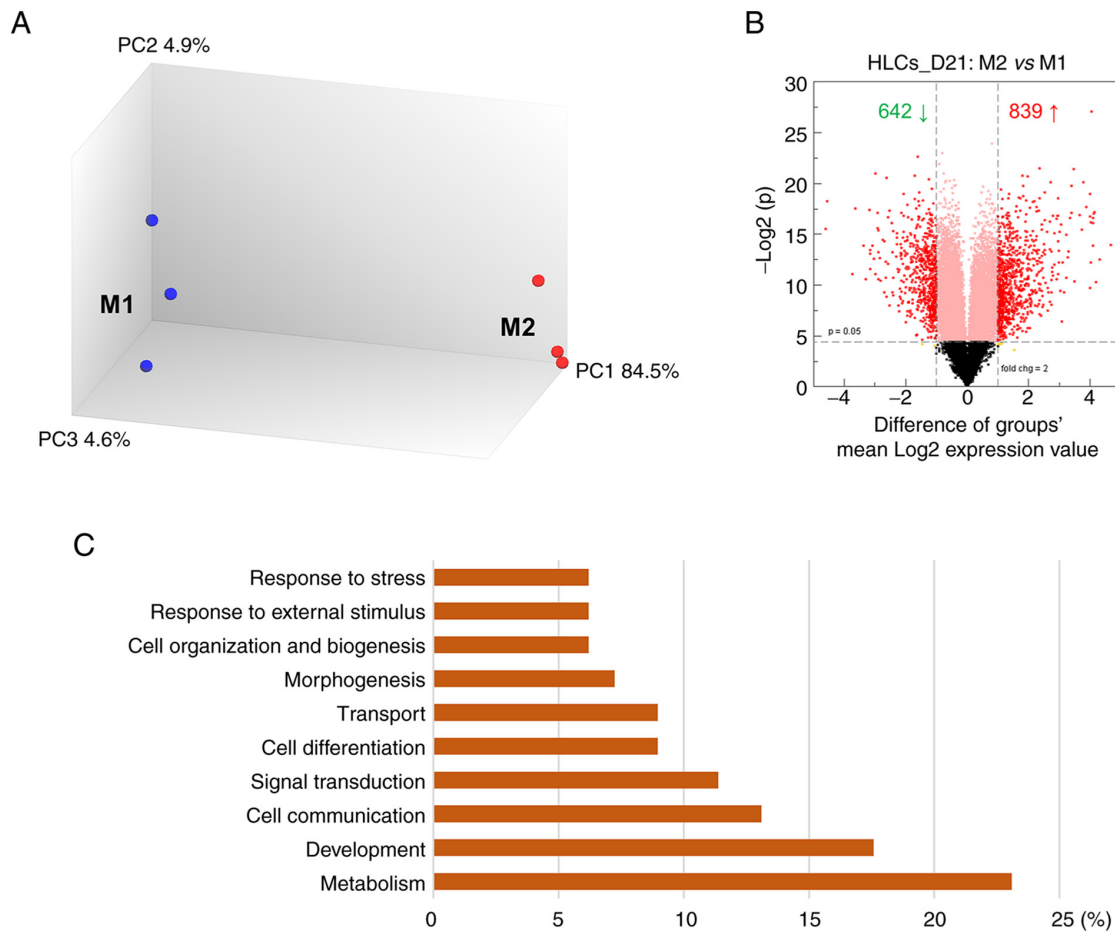
Figure 6. Comparison of HLCs on day 21 (D21) between differentiation Method 1 (M1) and Method 2 (M2). (A) Principal component analysis based on all probe sets. (B) Volcano plots showing the DEGs between HLCs (D21) from differentiation M1 and M2. All DEGs are shown as red dots. Downregulated genes are on the top-left corner with numbers denoted by green arrow, and upregulated genes are on the top-right corner denoted by red arrow. (C) Top 10 functional classes associated with the DEGs between two differentiation methods. HLC, hepatocyte-like cell; PC, principal component; DEG, differentially expressed gene.

To determine whether extended culture (beyond day 17) could improve the maturation of the HLCs, gene expression in HLCs between day 21 and 17 for both methods were compared. The results demonstrated that only 173 genes exhibited altered expression between days 17 and 21 in Method 1, with 140 upregulated and 33 downregulated genes. In contrast, 942 genes exhibited altered expression between days 17 and 21 in Method 2, including 381 upregulated and 561 downregulated genes (Fig. 5C). These results suggest that extended cell culture after day 17 further promoted HLC maturation in differentiation Method 2, but less so in Method 1.

Further comparison of gene expression in HLCs on day 21 from both methods to PHHs revealed substantial differences between HLCs and PHHs. In total, 14,595 DEGs were identified between HLCs generated from Method 1 and PHHs. Similarly, 12,537 DEGs were found between HLCs generated from Method 2 and PHHs (Fig. 5D). The numbers of the DEGs suggest that HLCs generated from Method 2 were slightly better than those generated from Method 1 (12,537 vs. 14,595 DEGs).

To further compare HLCs generated from the two differentiation methods, PCA was performed among the cell samples on day 21. As shown in Fig. 6A, the cell samples generated from differentiation Method 1 and 2 were well separated along the PC1 axis, accounting for 84.5% of the total variation. In total, 1,481 DEGs were identified between the two methods, with 839 genes upregulated and 642 downregulated (Method 2 vs. Method 1; Fig. 6B).

Functional and pathway analysis of the DEGs between the two differentiation methods. To elucidate cellular functions impacted by the DEGs between the two differentiation methods, the DEGs were annotated using DAVID to find GO terms overrepresented in the BP category. The 1,481 DEGs between the cell samples generated from the two methods on day 21 resulted in a total of 290 GO terms. Using the CateGOrizer online tool, these GO terms were further categorized into 34 functional classes within the pre-defined set of parent/ancestor GO terms. Fig. 6C shows the top 10 functional classes associated with the 1,481 DEGs, in which 'metabolism' was on top of the list, followed by 'development'. The other functional classes included 'cell communication', 'signal transduction', 'cell differentiation', 'transport', 'morphogenesis', 'cell organization and biogenesis', 'response to external stimulus' and 'response to stress'.

KEGG pathway analysis was performed to explore the molecular basis of the differences between the two hepatocyte differentiation methods. Several KEGG pathways that are

Table I. List of KEGG pathways enriched by the DEGs between the two differentiation methods that are closely involved in hepatocyte differentiation of pluripotent stem cells.

KEGG pathway	Number of DEGs	Percentage	Fold enrichment	P-value
ECM-receptor interaction	15	1.6	3.0	<0.0001
TGF-beta signaling pathway	13	1.4	2.7	0.003
Focal adhesion	23	2.5	2.0	0.003
Cytokine-cytokine receptor interaction	24	2.6	1.7	0.010
Hematopoietic cell lineage	11	1.2	2.2	0.024
Signaling pathways regulating pluripotency of stem cells	14	1.5	1.8	0.053
PI3K-Akt signaling pathway	27	2.9	1.4	0.080
Wnt signaling pathway	13	1.4	1.7	0.090

KEGG, Kyoto Encyclopedia of Genes and Genomes; DEG, differentially expressed genes; ECM extracellular matrix.
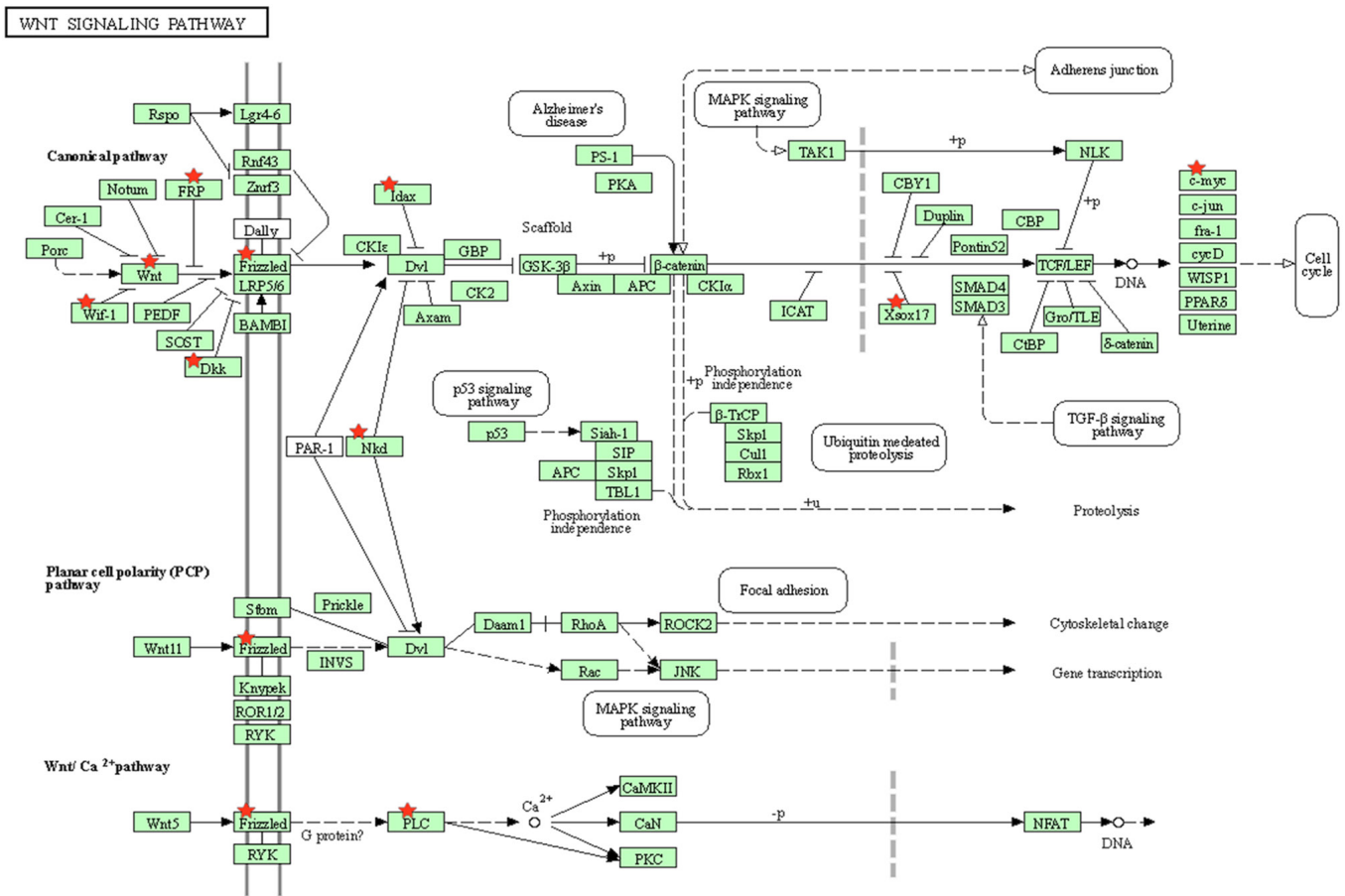
Figure 7. Wnt signaling pathway. Differentially expressed genes identified between the two differentiation methods are highlighted with red stars.

closely involved in hepatocyte differentiation of pluripotent stem cells were enriched by the 1,481 DEGs (Table I), including 'signaling pathways regulating pluripotency of stem cells', 'Wnt signaling pathway', 'TGF-beta signaling pathway' and 'PI3K-Akt signaling pathway'. The Wnt signaling pathway, which is closely involved in cell fate specification during hepatocyte differentiation of stem cells, is shown in Fig. 7. A total of 13 DEGs identified between the two differentiation methods were involved in the pathway, including CXXC4, SOX17, WIF1, WNT2, DKK1, DKK2, FZD1, FZD3, NKD1, PLCB4, SFRP2, SFRP5 and MYC, which are highlighted in the Fig. 7.

Discussion

Through phenotypical, functional and transcriptomic comparison of the two modified hepatocyte differentiation methods, which were based on existing well-known strategies, a stepwise improved method was established (shown in Fig. 1C, Method 2) that enabled efficient and reproducible differentiation of human iPSCs into homogeneous functional HLCs. Several factors contributed to the high efficiency, reproducibility and the homogeneity of the method: i) The use of a Cellartis DEF-CS single-cell culture system for the culture of iPSCs provided homogeneous starting cells with a high degree of pluripotency; ii) the use of the STEMdiff Definitive Endoderm kit, combined with the Cellartis DEF-CS single-cell culture system provided robust induction of pure and homogeneous DE cells; iii) Single-cell dissociation and re-plating of DE cells before initiating hepatic specification allowed for a homogeneous cell population for hepatocyte differentiation and a more flexible cell culture format for downstream applications; iv) DMSO combined with a high concentration of HGF, guided highly efficient and homogeneous hepatic specification; and v) further treatment with DEX, dihexa and OSM promoted cell maturation into functional HLCs.

Single-cell culture of iPSCs in the Cellartis DEF-CS culture system served as a key prerequisite for subsequent homogeneous hepatocyte differentiation. Heterogeneity of iPSCs, in terms of their morphology, self-renewal ability, pluripotency, differentiation bias and other traits, represents one of the critical challenges facing the stem cell field (29). To achieve efficient and reproducible cell differentiation, researchers have explored different strategies to improve the quality and homogeneity of starting iPSCs through optimizing the culture conditions of iPSCs and deriving new pluripotent cell types, such as naive iPSCs (30). Several reports indicated that dissociating the colony-type culture of iPSCs into a single-cell suspension for cell seeding improved DE differentiation (10,11,19). For example, in one study, by switching the cell culture of iPSCs from colony type to single-cell type, the percentage of DE cells expressing SOX17 and FOXA2 increased from 60-80% to 98% (10). However, the cells tended to form colonies upon removal of ROCK inhibitor from the cell culture medium, thus diminishing the potential of homogeneous cell differentiation. Single-cell culture without colony formation is a recently developed method for stem cell culture (31,32). Compared with conventional colony culture, it has the advantages of greater scalability, more rapid expansion and higher efficiency (31). The use of iPSCs maintained in single-cell culture has been reported to allow better and more homogeneous passage of the cells at the pluripotent stage (10). In this study, iPSCs were cultured in the Cellartis DEF-CS single-cell stem cell culture system and a highly homogeneous iPSC population was achieved to initiate DE induction, which laid a solid foundation for downstream HLC differentiation.

DE induction from iPSCs represents a critical step for subsequent efficient hepatic differentiation (33). Current approaches mostly rely on treatment either with growth factors such as activin A, FGFs and BMPs, or with CHIR99021, a small molecule GSK-3β inhibitor acting as a Wnt agonist (8,33). However, most of the methods showed high variability in DE induction, probably due to heterogeneity of the starting iPSCs, variability of growth factor activity and different sensitivities of cell lines to the induction reagents (10,12). Consequently, without fine-tuning the concentrations of growth factors or small molecules and adjusting the treatment timeline, it generally leads to non-homogeneous induction of SOX17$^+$/FOXA2$^+$ cells (10). To circumvent this hurdle, the STEMdiff Definitive Endoderm kit was tested on the single-cell culture of iPSCs. This kit has shown consistency and reproducibility in traditional colony-type culture of iPSCs (10). Robust DE induction was achieved from the single-cell culture of iPSCs maintained in the Cellartis DEF-CS culture system, as evidenced by the homogeneous spiky DE cell morphology, high expression of SOX17 and FOXA2 hepatic markers, and negative expression of OCT4 pluripotency marker. In addition, there was no apparent cell death during the DE induction from the single-cell culture of iPSCs. This observation differed from DE differentiation initiated from colony-type culture of iPSCs, where a large number of cells died and came off the surface of the tissue culture plates at the initial stage of DE induction (data not shown), likely due to Activin A or inhibitors of the PI3K pathway in the induction medium (34). These results indicate a higher homogeneity of the resultant DE cells and suggest iPSCs in single-cell culture as a more suitable state than colony-type culture for DE specification.

Upon successful DE formation, cell differentiation was next directed towards hepatic specification through two modified methods. Although starting from the same source of DE cells, considerable differences were observed during the differentiation process and in the final differentiated HLCs between these two methods, including cell morphology, differentiation efficiency, homogeneity and functional characteristics. Unlike cells from Method 1, which only displayed relatively mild cell morphological changes and showed an immature hepatic phenotype at the end of the differentiation, cells undergoing the differentiation process of Method 2 demonstrated significant morphological changes toward a final cell morphology closely resembling that of PHHs. Early studies have shown that there is an inverse relationship between cell proliferation and differentiation. Precursor cells continue dividing before acquiring a fully differentiated state, while terminal differentiation usually coincides with proliferation arrest and exit from the division cycle (35). This phenomenon might be explained by the massive cell growth observed in the hepatic specification and maturation process of Method 1, possibly due to insulin and other growth factors, such as FGF2 and HGF in the differentiation medium. A high rate of cell proliferation was also observed at the beginning of the hepatic specification in Method 2. However, the cells exhibited arrested growth after reaching confluency and switched to cell maturation thereafter. This finding emphasized the importance of coordinating cell proliferation and differentiation at the hepatic maturation stage to achieve functional HLCs. Significantly higher levels of protein expression of hepatic markers were detected in HLCs obtained from Method 2. Moreover, these cells demonstrated a substantially higher level of hepatic functionalities, including serum protein secretion, urea synthesis and release, and inducible CYP450 activity, which is essential for drug metabolism and hepatotoxicity studies. Taken together, these results demonstrate that in addition to the single-cell culture of homogeneous iPSCs and efficient DE induction, highly robust

hepatic specification and maturation represented another critical step toward highly efficient differentiation of homogeneous functional HLCs.

The present study showed that DMSO, combined with a high concentration of HGF, was capable of guiding highly efficient and homogeneous hepatic specification. DMSO has been used in previous studies, either separately or with cytokines/growth factors, for multiple lineage differentiation, including hepatic differentiation (36), although its specific mechanisms of action are still under investigation (36-39). It was reported that a hepatic specification step in the presence of DMSO allows for more homogeneous hepatocyte differentiation (10). However, subsets of undifferentiated stem cells remaining within the DE population may differentiate into other cell types in the presence of DMSO (40). This finding emphasizes the importance of a pure DE cell population before initiating hepatic specification. HGF is a multifunctional growth factor essential for liver development (33) and liver regeneration (41). It has been used in several growth factor-driven hepatocyte differentiation protocols (5,8,10). In the present study, 100 ng/ml HGF was used in conjunction with 1% DMSO; robust hepatic specification was obtained, as evidenced by the rapid change in cell morphology from spiky DE cells to polygonal hepatic cells, apparent intercellular junctions, lipid droplets across the cytoplasm and the upregulated expression of HNF4A in the differentiated HLCs.

Following hepatic specification, further treatment of the cells with DEX, dihexa and OSM boosted cell maturation into functional HLCs. The role of DEX in hepatic maturation has been well established (8). It has been shown to stabilize hepatocyte morphology *in vitro* by upregulating expression of adherens junction proteins (42), and to improve cytoskeletal arrangement and cell-cell contacts (43). DEX also upregulates the expression and the transcriptional activity of crucial liver transcription factors (44) and several hepatocyte-specific genes, including ALB, CYP2B (45,46) and CYP3A4 (47). Moreover, treatment with DEX alone induces maturation of hepatic progenitors towards hepatocytes that displayed characteristic nuclear staining of HNF4A and strong cytoplasmic expression of AFP, ALB and A1AT (10). Dihexa is an oligopeptide drug derived from angiotensin IV; it binds to HGF with a high affinity and in doing so potentiates its activity at its receptor, c-Met (48). To develop a small molecule-driven hepatocyte differentiation protocol, Siller *et al* (8) evaluated the effects of DEX and dihexa on hepatic progenitor cell maturation. They found that both DEX and dihexa were required to generate functional HLCs, and 100 nM of each compound provided the optimal results in terms of cell morphology and function of the final differentiated HLCs (8). OSM, a member of the IL-6 family, represents another distinct cytokine commonly used in hepatocyte maturation (2,5-7,46). Early studies found that fetal hepatocytes incubated with OSM display a similar morphology to mature hepatocytes (49). OSM upregulates the expression of several critical hepatic genes, including glucose-6-phosphatase, tyrosine aminotransferase and carbamoyl phosphate synthase in fetal hepatic cells (49,50). Furthermore, OSM induces multiple hepatocyte-specific functions, including glycogen synthesis, ammonia clearance, lipid synthesis and detoxification (46,50).

It is interesting to note that HLCs generated by Method 2 displayed the conspicuous formation of intracytoplasmic lipid droplets compared to those from Method 1. It is well established that the liver plays an important role in lipid metabolism, and hepatocytes store large amounts of lipid in the form of droplets for energy storage (51-53). The abundance of lipid droplets found in HLCs from Method 2 may suggest that these cells are highly active in lipid metabolism and storage. Intracellular lipid droplet formation was also observed in iPSC-derived HLCs reported by other groups (10,54,55). However, excessive lipid droplet formation may also indicate pathophysiological conditions, such as hepatic steatosis in nonalcoholic fatty liver disease caused by chronic exposure to environmental chemicals (56). Therefore, the nature of lipid droplet formation during hepatocyte differentiation of iPSCs should be further investigated. In addition, it must be pointed out that while the HLCs generated using this improved method (Method 2) expressed increased levels of hepatic markers and exhibited improved hepatic functionalities compared to cells derived from several existing growth factor- or small molecule-based hepatocyte differentiation protocols tested in our lab (data not shown), the relatively high expression of AFP in the final HLCs indicated that these cells still had a fetal phenotype. Therefore, additional efforts are required to further improve the maturation of the HLCs. Also, a relatively high concentration of HGF was utilized for efficient hepatic specification in this method, which has the disadvantage of increased cost. A lower level of HGF, in combination with dihexa or some other compounds that can potentiate the activity of HGF, should be considered for future studies.

Transcriptomic analysis allows for comprehensive assessment and unbiased comparison of biological samples. In addition to the phenotypical and functional studies described above, the HLCs generated from the two hepatocyte differentiation methods were further compared by whole genome gene expression profiling. HLCs generated from Method 2 were found to be slightly better than those generated from Method 1 in terms of the overall gene expression profile similarity to PHHs. However, regardless of the differentiation methods, vast differences existed between HLCs and PHHs, with >12,000 DEGs identified between HLCs and PHHs; very similar findings were reported by Godoy *et al* (57). Therefore, more effort is required to further improve the maturation of HLCs. Several approaches have been explored to enhance maturation of HLCs, including the formation of tissue-like 3D spheroids or organoids, use of extracellular matrix (ECM)-based hydrogels or scaffolds, coculture with endothelial cells or other hepatic cells, the addition of small molecules uncovered by screening, and overexpression of certain transcription factors, all of which are reviewed elsewhere (46). Nevertheless, the improvements on HLC maturation obtained using these methods are very limited. An improved understanding of the molecular and cellular basis of organogenesis of the liver coupled with emerging innovative technologies, such as 3D bioprinting (58), organ-on-chip microfluidics (59) and genome modification (60), may lead to breakthroughs in the field.

With this in mind, the current study explored the molecular basis underlying the differences observed between the two differentiation methods. Transcriptomic comparison of the HLCs derived by the two methods on day 21 identified 1,481 DEGs. Functional analysis of the DEGs revealed that,

in addition to 'metabolism', other functions such as 'development', 'cell communication', 'signal transduction' and 'cell differentiation' were associated with these DEGs, highlighting their involvement and influence on hepatocyte differentiation. Furthermore, pathway analysis of the DEGs identified several signaling pathways closely involved in hepatocyte differentiation of pluripotent stem cells. Among them, the 'ECM-receptor interaction' and 'focal adhesion pathways' play essential roles in cell proliferation, cell differentiation and cell survival, and are pivotal in tissue and organ morphogenesis (61). 'Signaling pathways regulating pluripotency of stem cells' coordinately promote self-renewal and pluripotency of pluripotent stem cells, but are disrupted upon initiation of hepatocyte differentiation (62). Moreover, the 'TGF-beta signaling pathway' regulates a broad spectrum of cellular functions such as proliferation, apoptosis, differentiation and migration (63). Of most interest is the 'Wnt signaling pathway' (Fig. 7). This pathway regulates basic developmental processes, such as cell-fate specification, progenitor-cell proliferation and the control of asymmetric cell division (64). More importantly, Wnt signaling is closely involved in cell fate specification during hepatocyte differentiation of stem cells (52). It was found that 13 genes involved in the pathway were differentially expressed between cells generated by the two methods, including Wnt (WNT2), its receptors (FZD1 and FZD3), and their inhibitors (WIF1, DKK1 and DKK2), as well as a few downstream inhibitors (NKD1, SFRP2, SFRP5, CXXC4 and SOX17). The altered expression of these key genes in the pathway is expected to have an impact on the pathway and affect the outcomes of hepatocyte differentiation.

In conclusion, based on the phenotypical, functional and transcriptomic comparison of the two modified hepatocyte differentiation methods, an improved method for efficient generation of homogeneous functional hepatocytes from iPSCs was developed. Compared with the HLCs derived from existing protocols evaluated in our group, the final differentiated HLCs derived from this enhanced method were highly homogeneous, both phenotypically and functionally. Combining the easy scale-up of the DEF-CS single-cell culture system for iPSCs, the highly efficient DE induction by the STEMdiff Definitive Endoderm kit, the robust hepatic specification guided by DMSO and HGF, and the hepatocyte maturation promoted by DEX, dihexa and OSM, this improved method may allow for robust generation of homogeneous functional hepatocytes from human stem cells and opens up new possibilities for drug discovery, hepatotoxicity studies and liver regenerative therapy. Moreover, the results of the transcriptomics analysis provide a molecular basis for the differences observed between the two differentiation methods, offer new insight into gene regulation in hepatogenesis *in vitro* and suggest ways to further improve hepatocyte differentiation in order to obtain more mature HLCs from human pluripotent stem cells for biomedical applications.

Availability of data and materials

The microarray dataset has been deposited in Gene Expression Omnibus (GEO; http://www.ncbi.nlm.nih.gov/geo/) of the National Center for Biotechnology Information with accession no. GSE187011. The datasets used and/or analyzed during the present study are also available from the corresponding author on reasonable request.

Authors' contributions

XG and RL conceived and designed the study, performed the experiments, analyzed the data and wrote the manuscript. RL performed the hepatocyte differentiation and the functional assays. XG performed the transcriptomic analysis. YZ analyzed the CYP assay samples using LC/MS. JJY and RLS contributed to the conception of the study, critically reviewed the manuscript. All authors read and approved the final manuscript. XG and RL confirmed the authenticity of all the raw data.

Ethics approval and consent to participate

Not applicable.

Patient consent for publication

Not applicable.

Competing interests

The authors declare that they have no competing interests.

References

1. Shi Y, Inoue H, Wu JC and Yamanaka S: Induced pluripotent stem cell technology: A decade of progress. Nat Rev Drug Discov 16: 115-130, 2017.
2. Hannoun Z, Steichen C, Dianat N, Weber A and Dubart-Kupperschmitt A: The potential of induced pluripotent stem cell derived hepatocytes. J Hepatol 65: 182-199, 2016.
3. Kogiso T, Nagahara H, Otsuka M, Shiratori K and Dowdy SF: Transdifferentiation of human fibroblasts into hepatocyte-like cells by defined transcriptional factors. Hepatol Int 7: 937-944, 2013.
4. Pournasr B, Asghari-Vostikolaee MH and Baharvand H: Transcription factor-mediated reprograming of fibroblasts to hepatocyte-like cells. Eur J Cell Biol 94: 603-610, 2015.
5. Mallanna SK and Duncan SA: Differentiation of hepatocytes from pluripotent stem cells. Curr Protoc Stem Cell Biol 26: 1G.4.1-1G.4.13, 2013.
6. Song Z, Cai J, Liu Y, Zhao D, Yong J, Duo S, Song X, Guo Y, Zhao Y, Qin H, *et al*: Efficient generation of hepatocyte-like cells from human induced pluripotent stem cells. Cell Res 19: 1233-1242, 2009.
7. Szkolnicka D, Farnworth SL, Lucendo-Villarin B and Hay DC: Deriving functional hepatocytes from pluripotent stem cells. Curr Protoc Stem Cell Biol 30: 1G.5.1-12, 2014.

8. Siller R, Greenhough S, Naumovska E and Sullivan GJ: Small-molecule-driven hepatocyte differentiation of human pluripotent stem cells. Stem Cell Reports 4: 939-952, 2015.

9. Du C, Feng Y, Qiu D, Xu Y, Pang M, Cai N, Xiang AP and Zhang Q: Highly efficient and expedited hepatic differentiation from human pluripotent stem cells by pure small-molecule cocktails. Stem Cell Res Ther 9: 58, 2018.

10. Carpentier A, Nimgaonkar I, Chu V, Xia Y, Hu Z and Liang TJ: Hepatic differentiation of human pluripotent stem cells in miniaturized format suitable for high-throughput screen. Stem Cell Res 16: 640-650, 2016.

11. Wang Y, Alhaque S, Cameron K, Meseguer-Ripolles J, Lucendo-Villarin B, Rashidi H and Hay DC: Defined and scalable generation of hepatocyte-like cells from human pluripotent stem cells. J Vis Exp: 55355, 2017.

12. Siller R and Sullivan GJ: Rapid screening of the endodermal differentiation potential of human pluripotent stem cells. Curr Protoc Stem Cell Biol 43: 1G.7.1-1G.7.23, 2017.

13. Corbett JL and Duncan SA: iPSC-derived hepatocytes as a platform for disease modeling and drug discovery. Front Med (Lausanne) 6: 265, 2019.

14. Takayama K and Mizuguchi H: Generation of human pluripotent stem cell-derived hepatocyte-like cells for drug toxicity screening. Drug Metab Pharmacokinet 32: 12-20, 2017.

15. Gao X, Yourick JJ and Sprando RL: Generation of nine induced pluripotent stem cell lines as an ethnic diversity panel. Stem Cell Res 31: 193-196, 2018.

16. Jung J, Zheng M, Goldfarb M and Zaret KS: Initiation of mammalian liver development from endoderm by fibroblast growth factors. Science 284: 1998-2003, 1999.

17. Basma H, Soto-Gutiérrez A, Yannam GR, Liu L, Ito R, Yamamoto T, Ellis E, Carson SD, Sato S, Chen Y, et al: Differentiation and transplantation of human embryonic stem cell-derived hepatocytes. Gastroenterology 136: 990-999, 2009.

18. Schneider CA, Rasband WS and Eliceiri KW: NIH image to imageJ: 25 Years of image analysis. Nat Methods 9: 671-675, 2012.

19. Asplund A, Pradip A, van Giezen M, Aspegren A, Choukair H, Rehnström M, Jacobsson S, Ghosheh N, El Hajjam D, Holmgren S, et al: One standardized differentiation procedure robustly generates homogenous hepatocyte cultures displaying metabolic diversity from a large panel of human pluripotent stem cells. Stem Cell Rev Rep 12: 90-104, 2016.

20. Gao X, Li R, Sprando RL and Yourick JJ: Concentration-dependent toxicogenomic changes of silver nanoparticles in hepatocyte-like cells derived from human induced pluripotent stem cells. Cell Biol Toxicol 37: 245-259, 2021.

21. Gao X, Li R, Cahan P, Zhao Y, Yourick JJ and Sprando RL: Hepatocyte-like cells derived from human induced pluripotent stem cells using small molecules: Implications of a transcriptomic study. Stem Cell Res Ther 11: 393, 2020.

22. Irizarry RA, Hobbs B, Collin F, Beazer-Barclay YD, Antonellis KJ, Scherf U and Speed TP: Exploration, normalization, and summaries of high density oligonucleotide array probe level data. Biostatistics 4: 249-264, 2003.

23. Fang H, Harris SC, Su Z, Chen M, Qian F, Shi L, Perkins R and Tong W: ArrayTrack: An FDA and public genomic tool. Methods Mol Biol 1613: 333-353, 2017.

24. Dennis G Jr, Sherman BT, Hosack DA, Yang J, Gao W, Lane HC and Lempicki RA: DAVID: Database for annotation, visualization, and integrated discovery. Genome Biol 4: P3, 2003.

25. Huang DW, Sherman BT, Tan Q, Kir J, Liu D, Bryant D, Guo Y, Stephens R, Baseler MW, Lane HC and Lempicki RA: DAVID bioinformatics resources: Expanded annotation database and novel algorithms to better extract biology from large gene lists. Nucleic Acids Res 35 (Web Server Issue): W169-W175, 2007.

26. Chen G, Gulbranson DR, Hou Z, Bolin JM, Ruotti V, Probasco MD, Smuga-Otto K, Howden SE, Diol NR, Propson NE, et al: Chemically defined conditions for human iPSC derivation and culture. Nat Methods 8: 424-429, 2011.

27. Esteves F, Rueff J and Kranendonk M: The central role of cytochrome p450 in xenobiotic metabolism-a brief review on a fascinating enzyme family. J Xenobiot 11: 94-114, 2021.

28. Guengerich FP: Common and uncommon cytochrome P450 reactions related to metabolism and chemical toxicity. Chem Res Toxicol 14: 611-650, 2001.

29. Hayashi Y, Ohnuma K and Furue MK: Pluripotent stem cell heterogeneity. Adv Exp Med Biol 1123: 71-94, 2019.

30. Weinberger L, Ayyash M, Novershtern N and Hanna JH: Dynamic stem cell states: Naive to primed pluripotency in rodents and humans. Nat Rev Mol Cell Biol 17: 155-169, 2016.

31. Chen KG, Mallon BS, Hamilton RS, Kozhich OA, Park K, Hoeppner DJ, Robey PG and McKay RD: Non-colony type monolayer culture of human embryonic stem cells. Stem Cell Res 9: 237-248, 2012.

32. Kunova M, Matulka K, Eiselleova L, Salykin A, Kubikova I, Kyrylenko S, Hampl A and Dvorak P: Adaptation to robust monolayer expansion produces human pluripotent stem cells with improved viability. Stem Cells Transl Med 2: 246-254, 2013.

33. Bogacheva MS, Khan S, Kanninen LK, Yliperttula M, Leung AW and Lou YR: Differences in definitive endoderm induction approaches using growth factors and small molecules. J Cell Physiol 233: 3578-3589, 2018.

34. McLean AB, D'Amour KA, Jones KL, Krishnamoorthy M, Kulik MJ, Reynolds DM, Sheppard AM, Liu H, Xu Y, Baetge EE and Dalton S: Activin a efficiently specifies definitive endoderm from human embryonic stem cells only when phosphatidylinositol 3-kinase signaling is suppressed. Stem Cells 25: 29-38, 2007.

35. Ruijtenberg S and van den Heuvel S: Coordinating cell proliferation and differentiation: Antagonism between cell cycle regulators and cell type-specific gene expression. Cell Cycle 15: 196-212, 2016.

36. Duan Y, Ma X, Zou W, Wang C, Bahbahan IS, Ahuja TP, Tolstikov V and Zern MA: Differentiation and characterization of metabolically functioning hepatocytes from human embryonic stem cells. Stem Cells 28: 674-686, 2010.

37. Baxter MA, Rowe C, Alder J, Harrison S, Hanley KP, Park BK, Kitteringham NR, Goldring CE and Hanley NA: Generating hepatic cell lineages from pluripotent stem cells for drug toxicity screening. Stem Cell Res 5: 4-22, 2010.

38. Rogler LE: Selective bipotential differentiation of mouse embryonic hepatoblasts in vitro. Am J Pathol 150: 591-602, 1997.

39. Czysz K, Minger S and Thomas N: DMSO efficiently down regulates pluripotency genes in human embryonic stem cells during definitive endoderm derivation and increases the proficiency of hepatic differentiation. PLoS One 10: e0117689, 2015.

40. Hay DC, Zhao D, Fletcher J, Hewitt ZA, McLean D, Urruticoechea-Uriguen A, Black JR, Elcombe C, Ross JA, Wolf R and Cui W: Efficient differentiation of hepatocytes from human embryonic stem cells exhibiting markers recapitulating liver development in vivo. Stem Cells 26: 894-902, 2008.

41. Michalopoulos GK: Principles of liver regeneration and growth homeostasis. Compr Physiol 3: 485-513, 2013.

42. Matsui T, Kinoshita T, Morikawa Y, Tohya K, Katsuki M, Ito Y, Kamiya A and Miyajima A: K-Ras mediates cytokine-induced formation of E-cadherin-based adherens junctions during liver development. EMBO J 21: 1021-1030, 2002.

43. Ren P, de Feijter AW, Paul DL and Ruch RJ: Enhancement of liver cell gap junction protein expression by glucocorticoids. Carcinogenesis 15: 1807-1813, 1994.

44. Fraczek J, Bolleyn J, Vanhaecke T, Rogiers V and Vinken M: Primary hepatocyte cultures for pharmaco-toxicological studies: At the busy crossroad of various anti-dedifferentiation strategies. Arch Toxicol 87: 577-610, 2013.

45. Schuetz EG, Schmid W, Schutz G, Brimer C, Yasuda K, Kamataki T, Bornheim L, Myles K and Cole TJ: The glucocorticoid receptor is essential for induction of cytochrome P-4502B by steroids but not for drug or steroid induction of CYP3A or P-450 reductase in mouse liver. Drug Metab Dispos 28: 268-278, 2000.

46. Chen C, Soto-Gutierrez A, Baptista PM and Spee B: Biotechnology challenges to in vitro maturation of hepatic stem cells. Gastroenterology 154: 1258-1272, 2018.

47. McCune JS, Hawke RL, LeCluyse EL, Gillenwater HH, Hamilton G, Ritchie J and Lindley C: In vivo and in vitro induction of human cytochrome P4503A4 by dexamethasone. Clin Pharmacol Ther 68: 356-366, 2000.

48. Benoist CC, Kawas LH, Zhu M, Tyson KA, Stillmaker L, Appleyard SM, Wright JW, Wayman GA and Harding JW: The procognitive and synaptogenic effects of angiotensin IV-derived peptides are dependent on activation of the hepatocyte growth factor/c-met system. J Pharmacol Exp Ther 351: 390-402, 2014.

49. Kamiya A, Kinoshita T, Ito Y, Matsui T, Morikawa Y, Senba E, Nakashima K, Taga T, Yoshida K, Kishimoto T and Miyajima A: Fetal liver development requires a paracrine action of oncostatin M through the gp130 signal transducer. EMBO J 18: 2127-2136, 1999.

50. Kamiya A, Kinoshita T and Miyajima A: Oncostatin M and hepatocyte growth factor induce hepatic maturation via distinct signaling pathways. FEBS Lett 492: 90-94, 2001.
51. Mashek DG: Hepatic lipid droplets: A balancing act between energy storage and metabolic dysfunction in NAFLD. Mol Metab 50: 101115, 2021.
52. Gordillo M, Evans T and Gouon-Evans V: Orchestrating liver development. Development 142: 2094-2108, 2015.
53. Nguyen P, Leray V, Diez M, Serisier S, Le Bloc'h J, Siliart B and Dumon H: Liver lipid metabolism. J Anim Physiol Anim Nutr (Berl) 92: 272-283, 2008.
54. Mathapati S, Siller R, Impellizzeri AA, Lycke M, Vegheim K, Almaas R and Sullivan GJ: Small-Molecule-Directed Hepatocyte-Like Cell Differentiation of Human Pluripotent stem cells. Curr Protoc Stem Cell Biol 38: 1G.6.1-1G.6.18, 2016.
55. Kiamehr M, Alexanova A, Viiri LE, Heiskanen L, Vihervaara T, Kauhanen D, Ekroos K, Laaksonen R, Käkelä R and Aalto-Setälä K: hiPSC-derived hepatocytes closely mimic the lipid profile of primary hepatocytes: A future personalised cell model for studying the lipid metabolism of the liver. J Cell Physiol 234: 3744-3761, 2019.
56. Zheng S, Yang Y, Wen C, Liu W, Cao L, Feng X, Chen J, Wang H, Tang Y, Tian L, *et al*: Effects of environmental contaminants in water resources on nonalcoholic fatty liver disease. Environ Int 154: 106555, 2021.
57. Godoy P, Schmidt-Heck W, Natarajan K, Lucendo-Villarin B, Szkolnicka D, Asplund A, Björquist P, Widera A, Stöber R, Campos G, *et al*: Gene networks and transcription factor motifs defining the differentiation of stem cells into hepatocyte-like cells. J Hepatol 63: 934-942, 2015.
58. Faulkner-Jones A, Fyfe C, Cornelissen DJ, Gardner J, King J, Courtney A and Shu W: Bioprinting of human pluripotent stem cells and their directed differentiation into hepatocyte-like cells for the generation of mini-livers in 3D. Biofabrication 7: 044102, 2015.
59. Beckwitt CH, Clark AM, Wheeler S, Taylor DL, Stolz DB, Griffith L and Wells A: Liver 'organ on a chip'. Exp Cell Res 363: 15-25, 2018.
60. Xie Y, Yao J, Jin W, Ren L and Li X: Induction and maturation of hepatocyte-like cells in vitro: Focus on technological advances and challenges. Front Cell Dev Biol 9: 765980, 2021.
61. Walker C, Mojares E and Del Río Hernández A: Role of extracellular matrix in development and cancer progression. Int J Mol Sci 19: 3028, 2018.
62. Okita K and Yamanaka S: Intracellular signaling pathways regulating pluripotency of embryonic stem cells. Curr Stem Cell Res Ther 1: 103-111, 2006.
63. Itoh F, Watabe T and Miyazono K: Roles of TGF-β family signals in the fate determination of pluripotent stem cells. Semin Cell Dev Biol 32: 98-106, 2014.
64. Bielen H and Houart C: The Wnt cries many: Wnt regulation of neurogenesis through tissue patterning, proliferation, and asymmetric cell division. Dev Neurobiol 74: 772-780, 2014.